

University of Groningen

Study of the $f_0(980)$ and $f_0(500)$ Scalar Mesons through the Decay $D_s^+ \rightarrow \pi^+\pi^-e^+\nu_e$

BESIII Collaboration; Kalantar-Nayestanaki, N.; Kappert, R.; Kavatsyuk, M.; Messchendorp, J.; Rodin, V.

Published in:
Physical Review Letters

DOI:
[10.1103/PhysRevLett.132.141901](https://doi.org/10.1103/PhysRevLett.132.141901)

IMPORTANT NOTE: You are advised to consult the publisher's version (publisher's PDF) if you wish to cite from it. Please check the document version below.

Document Version
Publisher's PDF, also known as Version of record

Publication date:
2024

[Link to publication in University of Groningen/UMCG research database](#)

Citation for published version (APA):

BESIII Collaboration, Kalantar-Nayestanaki, N., Kappert, R., Kavatsyuk, M., Messchendorp, J., & Rodin, V. (2024). Study of the $f_0(980)$ and $f_0(500)$ Scalar Mesons through the Decay $D_s^+ \rightarrow \pi^+\pi^-e^+\nu_e$. *Physical Review Letters*, 132(14), Article 141901. <https://doi.org/10.1103/PhysRevLett.132.141901>

Copyright

Other than for strictly personal use, it is not permitted to download or to forward/distribute the text or part of it without the consent of the author(s) and/or copyright holder(s), unless the work is under an open content license (like Creative Commons).

The publication may also be distributed here under the terms of Article 25fa of the Dutch Copyright Act, indicated by the "Taverne" license. More information can be found on the University of Groningen website: <https://www.rug.nl/library/open-access/self-archiving-pure/taverne-amendment>.


Take-down policy

If you believe that this document breaches copyright please contact us providing details, and we will remove access to the work immediately and investigate your claim.

Downloaded from the University of Groningen/UMCG research database (Pure): <http://www.rug.nl/research/portal>. For technical reasons the number of authors shown on this cover page is limited to 10 maximum.

Study of the $f_0(980)$ and $f_0(500)$ Scalar Mesons through the Decay $D_s^+ \rightarrow \pi^+ \pi^- e^+ \nu_e$

M. Ablikim *et al.**
(BESIII Collaboration)

 (Received 23 March 2023; revised 29 November 2023; accepted 28 February 2024; published 5 April 2024)

Using e^+e^- collision data corresponding to an integrated luminosity of 7.33 fb^{-1} recorded by the BESIII detector at center-of-mass energies between 4.128 and 4.226 GeV, we present an analysis of the decay $D_s^+ \rightarrow \pi^+ \pi^- e^+ \nu_e$, where the D_s^+ is produced via the process $e^+e^- \rightarrow D_s^{*\pm} D_s^\mp$. We observe the $f_0(980)$ in the $\pi^+ \pi^-$ system and the branching fraction of the decay $D_s^+ \rightarrow f_0(980) e^+ \nu_e$ with $f_0(980) \rightarrow \pi^+ \pi^-$ measured to be $(1.72 \pm 0.13_{\text{stat}} \pm 0.10_{\text{syst}}) \times 10^{-3}$, where the uncertainties are statistical and systematic, respectively. The dynamics of the $D_s^+ \rightarrow f_0(980) e^+ \nu_e$ decay are studied with the simple pole parametrization of the hadronic form factor and the Flatté formula describing the $f_0(980)$ in the differential decay rate, and the product of the form factor $f_+^{f_0}(0)$ and the $c \rightarrow s$ Cabibbo-Kobayashi-Maskawa matrix element $|V_{cs}|$ is determined for the first time to be $f_+^{f_0}(0)|V_{cs}| = 0.504 \pm 0.017_{\text{stat}} \pm 0.035_{\text{syst}}$. Furthermore, the decay $D_s^+ \rightarrow f_0(500) e^+ \nu_e$ is searched for the first time but no signal is found. The upper limit on the branching fraction of $D_s^+ \rightarrow f_0(500) e^+ \nu_e$, $f_0(500) \rightarrow \pi^+ \pi^-$ decay is set to be 3.3×10^{-4} at 90% confidence level.

DOI: [10.1103/PhysRevLett.132.141901](https://doi.org/10.1103/PhysRevLett.132.141901)

Introduction.—Quantum chromodynamics (QCD), the fundamental theory of the strong interaction, has been established for almost half a century. However, there are some features that still need to be understood, such as quark confinement and dynamics in the nonperturbative regime. The light scalar mesons $f_0(500)$, $f_0(980)$, and $a_0(980)$ play a crucial role in the dynamics of the spontaneous breaking of QCD chiral symmetry and in the origin of pseudoscalar meson masses [1,2], and consequently can be used to probe the confinement of quarks [3]. Furthermore, our understanding of the nature of light hadrons is still poor since QCD is nonperturbative in the low-energy region. Investigating the structure of the light scalar mesons provides key input to these issues. In spite of the striking success of the constituent quark model, the nontrivial quark structure of these mesons has remained controversial for many years [4]. Their mass ordering cannot be explained by a $q\bar{q}$ configuration in the naive quark model, leaving open the possibility that they are mixtures of $q\bar{q}$ states [3,5–15]. Other interpretations are diquark-antidiquark states (tetraquark) [16] and meson-meson bound states (molecule) [17]. Therefore, more conclusive experimental measurements of these scalar states are highly desired.

Since the leptons and hadrons in the final state interact only weakly with each other, semileptonic decays of charm mesons provide a unique and clean platform to probe the constituent $q\bar{q}$ components in the wave functions of light scalar states [18]. Here, only the spectator light quarks are related to the formation of these states and the quark flavor content can be specified through Cabibbo-favored and -suppressed processes [19]. Additionally, the dynamics of the semileptonic charmed meson decays can be studied by measuring the hadronic form factor that describes the strong interaction between the final-state quarks, including all the nonperturbative effects. This provides an excellent opportunity to test the different theoretical methods of solving the QCD nonperturbative problem. Since the form factors and branching fractions (BFs) of the semileptonic charmed meson decays are highly sensitive to the internal structure of light scalar states, studies of the dynamics of these decays are also important to understand their nature [12].

In previous studies, the BESIII Collaboration has reported measurements of the decays $D^{0(+)} \rightarrow a_0(980)^{-(0)} e^+ \nu_e$ [20], $D^+ \rightarrow f_0(500) e^+ \nu_e$ [21], and $D_s^+ \rightarrow f_0(980) e^+ \nu_e$ with $f_0(980) \rightarrow \pi^0 \pi^0$ [22], and searches of the decays $D^+ \rightarrow f_0(980) e^+ \nu_e$ [21], $D_s^+ \rightarrow a_0(980)^0 e^+ \nu_e$ [23], and $D_s^+ \rightarrow f_0(500) e^+ \nu_e$ with $f_0(500) \rightarrow \pi^0 \pi^0$ [22]. With negligible contamination from the $D_s^+ \rightarrow \rho^0 e^+ \nu_e$ channel, the decay $D_s^+ \rightarrow \pi^+ \pi^- e^+ \nu_e$ enables us to study the structure of $f_0(980)$ in a clean environment. Previously, only the CLEO Collaboration measured the BF of the decay $D_s^+ \rightarrow f_0(980) e^+ \nu_e$ with $f_0(980) \rightarrow \pi^+ \pi^-$ [24–26] with data taken at a center-of-mass (CM) energy (E_{CM}) near 4.170 GeV. With a data sample more than 10 times larger,

*Full author list given at the end of the Letter.

Published by the American Physical Society under the terms of the [Creative Commons Attribution 4.0 International license](https://creativecommons.org/licenses/by/4.0/). Further distribution of this work must maintain attribution to the author(s) and the published article's title, journal citation, and DOI. Funded by SCOAP³.

we report a significantly improved measurement of the BF and the first measurement of the transition form factor of the decay $D_s^+ \rightarrow f_0(980)e^+\nu_e$ with $f_0(980) \rightarrow \pi^+\pi^-$, and the first search of the decay $D_s^+ \rightarrow f_0(500)e^+\nu_e$ with $f_0(500) \rightarrow \pi^+\pi^-$. The obtained results are important tests of theoretical predictions based on different models [6–12,14,15]. Throughout this Letter, charge-conjugate channels are implied.

BESIII experiment and data samples.—For the BF measurements of semileptonic decays, we use the same tag technique of Refs. [22,23,27] with additional detail contained in Appendix A. Our measurements are performed based on e^+e^- collision data corresponding to an integrated luminosity of 7.33 fb^{-1} collected with the BESIII detector at $E_{\text{CM}} = 4.128\text{--}4.226 \text{ GeV}$ [28]. Details about the BESIII detector design and performance are provided in Refs. [29–31].

Simulated data samples produced with a GEANT4-based [32] Monte Carlo (MC) package, which includes the geometric description of the BESIII detector [33] and the detector response, are used to determine detection efficiencies and to estimate backgrounds. The simulation models the beam energy spread and initial state radiation in the e^+e^- annihilations with the generator KKMC [34]. The inclusive MC sample includes the production of open-charm processes, the initial state radiation production of vector charmonium(-like) states, and the continuum processes incorporated in KKMC [34]. All particle decays are modeled with EVTGEN [35] using BFs either taken from the Particle Data Group [4], when available, or otherwise estimated with LUNDCHARM [36]. Final state radiation from charged final state particles is incorporated using the PHOTOS package [37]. The signal detection efficiencies and signal shapes are obtained from the signal MC samples, in which the D_s^- decays inclusively to all known decay channels and the signal D_s^+ decays to $\pi^+\pi^-e^+\nu_e$ with the S -wave contribution simulated according to previous measurements [21,38]. The amplitudes for the $f_0(980)$ is modeled by the Flatté formula with its parameters fixed to the BESII measurement [39].

Event selection.—The tag D_s^- candidates are reconstructed with $K^\pm, \pi^\pm, \rho^-, \rho^0, \pi^0, \eta^{(\prime)}$, and K_S^0 mesons in 12 tag modes: $K^+K^-\pi^-, K_S^0K^-, \pi^-\eta, \pi^-\eta'_{\pi^+\pi^-}, K^+K^-\pi^-\pi^0, \pi^+\pi^-\pi^-, K_S^0K^+\pi^-\pi^-, \rho^-\eta, \pi^-\eta'_{\rho^0}, K^+\pi^-\pi^-, K_S^0K^-\pi^0$, and $K_S^0K^-\pi^+\pi^-$. A detailed description of the selection criteria for all tag candidates except $\rho^-\eta$ can be found in Ref. [40]. The ρ^- candidates are reconstructed from $\pi^-\pi^0$ combinations within an invariant mass interval $(0.625, 0.925) \text{ GeV}/c^2$. Requirements on the recoiling mass m_{rec} against the tag D_s^- candidates are applied to the tag candidates in order to identify the process $e^+e^- \rightarrow D_s^{*\pm}D_s^\mp$. If there are multiple candidates for a specific tag mode per charge, the one with m_{rec} closest to the known $D_s^{*\pm}$ mass [4] is chosen. For each tag mode, the

tag yield is extracted from the fit to the tag D_s^- mass spectrum ($M_{D_s^-}$). The signals are modeled with the MC-simulated signal shape convolved with a Gaussian function to account for the resolution difference between data and MC simulation, while the combinatorial backgrounds are parametrized with a first-order or second-order Chebyshev polynomial. For the tag mode $D_s^- \rightarrow K_S^0K^-$, the peaking background from $D^- \rightarrow K_S^0\pi^-$ decay is described by the MC-simulated shape that is smeared with the same Gaussian function as used in the signal, with the background yield determined from the fit. Summing over various tag modes and energy points, we obtain the total tag yield $N_{\text{tag}}^{\text{tot}} = 771101 \pm 3445$. For more details about tag candidates, such as selection regions and reconstruction efficiencies, see Ref. [28].

After a D_s^- candidate is identified, we reconstruct the decay $D_s^+ \rightarrow \pi^+\pi^-e^+\nu_e$ recoiling against the tag side, requiring three charged tracks identified as a $\pi^+\pi^-$ pair with the same selection criteria as on the tag side and e^+ (opposite sign to the tag D_s^-) following Ref. [41]. Using the same kinematic fit method of Refs. [27], we reconstruct the transition photon from the main decay $D_s^{*\pm} \rightarrow \gamma D_s^\pm$.

For the real $D_s^{*\pm}D_s^\mp$ events, the square of the recoiling mass (M_{rec}^2) against the transition photon and the tag D_s^- is expected to peak at the known D_s^+ mass squared. To improve the resolution, the decay products of the tag D_s^- are constrained to the known D_s^+ mass [4]. We require M_{rec}^2 to be within $(3.78, 4.05) \text{ GeV}^2/c^4$ to suppress the backgrounds from non- $D_s^{*\pm}D_s^\mp$ processes. The missing neutrino information is inferred by the missing mass squared, which is defined as

$$M_{\text{miss}}^2 = (\mathbf{p}_{\text{CM}} - \mathbf{p}_{\text{tag}} - \mathbf{p}_{\pi^+} - \mathbf{p}_{\pi^-} - \mathbf{p}_e - \mathbf{p}_\gamma)^2, \quad (1)$$

where \mathbf{p}_{CM} is the four-momentum of the e^+e^- center-of-mass system, \mathbf{p}_{tag} for the tag D_s^- , $\mathbf{p}_{\pi^+(\pi^-,e)}$ for the semileptonic final state, and \mathbf{p}_γ for the transition photon from the $D_s^{*\pm}$ decay. Here, the measured momenta of the tag D_s^- and the transition photon are corrected with the kinematic fit to improve the resolution. In order to further reject backgrounds, we require $|M_{\text{miss}}^2| < 0.06 \text{ GeV}^2/c^4$.

BF measurement.—To study the $f_0(980)$, we require the $\pi^+\pi^-$ invariant mass ($M_{\pi^+\pi^-}$, see Fig. 1) to be within the interval $(0.6, 1.6) \text{ GeV}/c^2$. The nonpeaking background distribution from the inclusive MC sample is verified using events from the data sideband region (about 2σ away from the signal region of the tag D_s^- mass and having the same interval as signal region) of the tag $M_{D_s^-}$ distribution. The peak around $0.77 \text{ GeV}/c^2$ is mainly caused by the decay $D_s^+ \rightarrow \eta'(\gamma\pi^+\pi^-)e^+\nu_e$. We find that the inclusive MC adequately describes the data in this channel. An unbinned maximum likelihood fit to the $M_{\pi^+\pi^-}$ distribution is performed to extract the signal yield of $D_s^+ \rightarrow f_0(980)e^+\nu_e$, $f_0(980) \rightarrow \pi^+\pi^-$ decay. In the fit, the signal is modeled

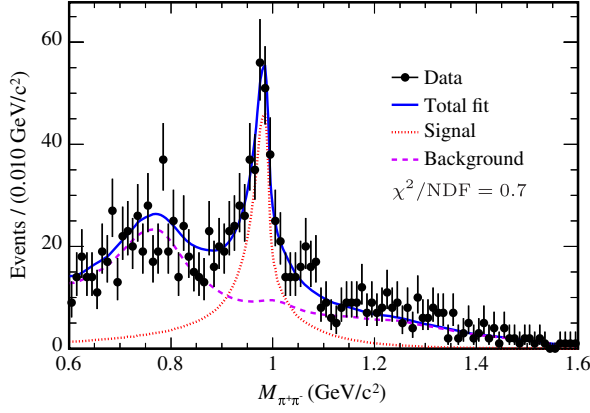


FIG. 1. Fit to the $M_{\pi^+\pi^-}$ distribution of the accepted candidates for the decay $D_s^+ \rightarrow f_0(980)e^+\nu_e$. The points with error bars are data, and the blue line is the total fit. The red dotted and violet dashed lines are the signal and background shapes, respectively.

with an MC-simulated line shape convolved with a Gaussian resolution function, and the background is described by the inclusive MC shape convolved with the same Gaussian function. From the fit, which is shown in Fig. 1, we obtain the total signal yield $N_{\text{sig}}^{\text{tot}} = 439 \pm 33$. The goodness of fit χ^2/NDF is 0.7, where NDF is the number of degrees of freedom. Particularly, the other S -wave contributions from the $f_0(500)$, $f_0(1370)$ and nonresonance can be ignored since no significant signal is observed. Using the $(35.44 \pm 0.07)\%$ weighted efficiency provided in Ref. [28] and the formula in Appendix A, we obtain $\mathcal{B}[D_s^+ \rightarrow f_0(980)e^+\nu_e, f_0(980) \rightarrow \pi^+\pi^-] = (1.72 \pm 0.13_{\text{stat}} \pm 0.10_{\text{syst}}) \times 10^{-3}$, where the systematic uncertainties are discussed in Appendix B. Using the BF $\mathcal{B}[f_0(980) \rightarrow \pi^+\pi^-] = (46 \pm 6)\%$ assuming the dominant $\pi\pi$ and KK decays [42] and the relation $\mathcal{B}[D_s^+ \rightarrow f_0(980)e^+\nu_e] = 4.22 \times 10^{-3} \cos^2\phi$ with the mixing angle ϕ involved in the $q\bar{q}$ mixture picture for $f_0(980)$ as $\sin\phi(1/\sqrt{2})(u\bar{u} + d\bar{d}) + \cos\phi s\bar{s}$ [8,11], we obtain the angle $\phi = (19.7 \pm 12.8)^\circ$ implying that the $s\bar{s}$ component dominates.

We further search for the decay $D_s^+ \rightarrow f_0(500)e^+\nu_e$ with $f_0(500) \rightarrow \pi^+\pi^-$. To avoid the background from $D_s^+ \rightarrow K_S^0 e^+\nu_e$ decay and the possible tail of $D_s^+ \rightarrow f_0(980)e^+\nu_e$ decay, we only use the events satisfying $M_{\pi^+\pi^-} < 0.45 \text{ GeV}/c^2$. The background yield of $D_s^+ \rightarrow f_0(980)e^+\nu_e$, $f_0(980) \rightarrow \pi^+\pi^-$ decay is estimated to be 5.4 based on the foregoing study. An unbinned maximum likelihood fit to the M_{miss}^2 distribution of the accepted candidates is performed, where the signal and background shapes are modeled by the simulated shapes obtained from the signal and inclusive MC samples, respectively. The fit result is shown in Fig. 2. Since no significant signal is observed, an upper limit on the BF at 90% confidence level with the $(11.98 \pm 0.06)\%$ weighted efficiency is set to be $\mathcal{B}[D_s^+ \rightarrow f_0(500)e^+\nu_e, f_0(500) \rightarrow \pi^+\pi^-] < 3.3 \times 10^{-4}$ following Ref. [22]. The related systematic uncertainties are discussed in Appendix B.

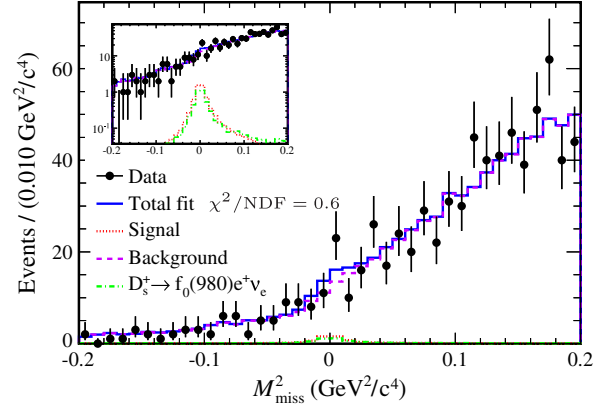


FIG. 2. Fit to the M_{miss}^2 distribution of the accepted candidates for $D_s^+ \rightarrow f_0(500)e^+\nu_e$ decay. The black points with error bars are data, and the blue line is the total fit. The red dotted and violet dashed lines are the signal and background shapes, respectively. The green dotted-dashed line is the decay $D_s^+ \rightarrow f_0(980)e^+\nu_e$.

Form factor measurement.—The dynamics of $D_s^+ \rightarrow f_0(980)e^+\nu_e$ decay is studied by dividing the semileptonic candidate events into four intervals of q^2 (four-momentum transfer square of $e^+\nu_e$). Using the measured and expected partial decay rates of the i th q^2 interval, $\Delta\Gamma_{\text{mea}}^i$ and $\Delta\Gamma_{\text{exp}}^i$, the form factor is determined by constructing and minimizing a χ^2 as

$$\chi^2 = \sum_{ij} (\Delta\Gamma_{\text{mea}}^i - \Delta\Gamma_{\text{exp}}^i) (C^{-1})_{ij} (\Delta\Gamma_{\text{mea}}^j - \Delta\Gamma_{\text{exp}}^j), \quad (2)$$

where C_{ij} is the covariance matrix to consider correlations of $\Delta\Gamma_{\text{mea}}^i$ among q^2 intervals.

The $\Delta\Gamma_{\text{exp}}^i$ is calculated by integrating the following double differential decay rate [43]:

$$\frac{d^2\Gamma(D_s^+ \rightarrow f_0(980)e^+\nu_e)}{dsdq^2} = \frac{G_F^2 |V_{cs}|^2}{192\pi^4 m_{D_s^+}^3} \lambda^{3/2}(m_{D_s^+}^2, s, q^2) \times |f_+^{f_0}(q^2)|^2 P(s), \quad (3)$$

where s is the square of $M_{\pi^+\pi^-}$, G_F is the Fermi constant [4], $|V_{cs}|$ is the Cabibbo-Kobayashi-Maskawa matrix element, $m_{D_s^+}$ is the known D_s^+ mass [4], $\lambda(x, y, z) = x^2 + y^2 + z^2 - 2xy - 2xz - 2yz$, and $P(s)$ is based on the relativistic Flatté formula [39] due to the open K^+K^- channel as follows:

$$P(s) = \frac{g_1 \rho_{\pi\pi}}{|m_0^2 - s - i(g_1 \rho_{\pi\pi} + g_2 \rho_{K\bar{K}})|^2}. \quad (4)$$

Here, m_0 denotes the $f_0(980)$ mass; the constants g_1 and g_2 are the $f_0(980)$ couplings to $\pi^+\pi^-$ and K^+K^- final states, respectively; and $\rho_{\pi\pi}$ and $\rho_{K\bar{K}}$ are individual phase space factors. Using the decay widths in the different q^2 intervals,

the form factor $|f_+^{f_0}(q^2)|$ can be extracted. In this Letter, the form factor is modeled with the simple pole parametrization [44]:

$$f_+^{f_0}(q^2) = \frac{f_+^{f_0}(0)}{1 - q^2/M_{\text{pole}}^2}, \quad (5)$$

where $f_+^{f_0}(0)$ is the form factor evaluated at $q^2 = 0$, and the pole mass $M_{\text{pole}} = 2.46 \text{ GeV}/c^2$ [4,45].

The measured partial decay rate $\Delta\Gamma_{\text{mea}}^i$ is determined by $\Delta\Gamma_{\text{mea}}^i \equiv \int_i \int_s (d^2\Gamma/dsdq^2) ds dq^2 = N_{\text{pro}}^i / (\tau N_{\text{tag}}^{\text{tot}} \mathcal{B}_\gamma)$, where \mathcal{B}_γ represents the BF of $D_s^{\pm} \rightarrow \gamma D_s^{\pm}$, τ is the D_s^+ meson lifetime [4,46], and N_{pro}^i is the signal yield produced in the i th q^2 interval, obtained as $N_{\text{pro}}^i = \sum_{j=1}^4 \epsilon_{ij}^{-1} N_{\text{obs}}^j$. Here, N_{obs}^j is the observed signal yield obtained from a fit to the $M_{\pi^+\pi^-}$ distribution in the j th q^2 interval, which is carried out in a similar manner as the one described previously for the BF measurement, and ϵ_{ij} is the efficiency matrix determined from the signal MC samples via $\epsilon_{ij} = \sum_k [(1/N_{\text{tag}}^{\text{tot}}) \times (N_{\text{rec}}^{ij}/N_{\text{gen}}^j)_k \times (N_{\text{tag}}^k/\epsilon_{\text{tag}}^k)]$, where N_{rec}^{ij} is the signal yield reconstructed in the i th q^2 interval and generated in the j th q^2 interval, N_{gen}^j is the total signal yield generated in the j th q^2 interval, and k sums over all tag modes. The details of the divisions, N_{obs}^i and $\Delta\Gamma_{\text{mea}}^i$ of various q^2 intervals are given in Ref. [28].

The statistical and systematic covariance matrices are constructed as $C_{ij}^{\text{stat}} = [1/(\tau N_{\text{tag}}^{\text{tot}})^2] \sum_\alpha \epsilon_{i\alpha}^{-1} \epsilon_{j\alpha}^{-1} \sigma^2(N_{\text{obs}}^\alpha)$ and $C_{ij}^{\text{syst}} = \delta(\Delta\Gamma_{\text{mea}}^i) \delta(\Delta\Gamma_{\text{mea}}^j)$, respectively, where $\sigma(N_{\text{obs}}^\alpha)$ and $\delta(\Delta\Gamma_{\text{mea}}^i)$ are the statistical and systematic uncertainties in the i th q^2 interval. The C_{ij}^{syst} is obtained by summing all the covariance matrices for all systematic uncertainties, where the systematic uncertainty of τ , 0.8% [4,46], is involved besides those in the BF measurement. The obtained C_{ij}^{stat} and C_{ij}^{syst} , the resulting $C_{ij} = C_{ij}^{\text{stat}} + C_{ij}^{\text{syst}}$, and the relevant correlation matrix element ρ_{ij} are shown in Ref. [28].

The systematic uncertainty related to $\Delta\Gamma_{\text{mea}}^i$ is estimated to be 2.6% by following Ref. [47]. In addition, the input parameters m_0 , g_1 , and g_2 [39] related to $\Delta\Gamma_{\text{exp}}^i$ are also considered by varying them within $\pm 1\sigma$ from their central values. The largest deviations of the form factor, respectively 2.2%, 1.2%, and 6.0%, are taken as systematic uncertainties. The quadrature sum of the above uncertainties is 6.9%, which is taken as the total systematic uncertainty.

The fit to the differential decay rate of the channel $D_s^+ \rightarrow f_0(980)e^+\nu_e$ and the form factor projection are shown in Fig. 3. Using the form factor parametrization of Eq. (3) and the Flatté formula Eq. (4) for the $f_0(980)$ decay in the fit, the product of the form factor and $|V_{cs}|$ is determined to be

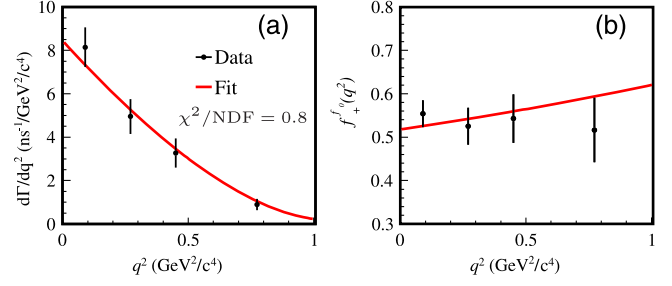


FIG. 3. Fit to the differential decay rate as a function of q^2 (a) and projection to the form factor $f_+^{f_0}(q^2)$ (b). The points with error bars are data, and the red line is the fit.

$f_+^{f_0}(0)|V_{cs}| = 0.504 \pm 0.017_{\text{stat}} \pm 0.035_{\text{syst}}$. The fit result is shown in Fig. 3(a), while Fig. 3(b) shows the same fit in projection to the form factor $f_+^{f_0}(q^2)$.

Summary and discussions.—Using e^+e^- collision data corresponding to an integrated luminosity of 7.33 fb^{-1} collected at $E_{\text{CM}} = 4.128\text{--}4.226 \text{ GeV}$ by the BESIII detector, we measure the BF of the decay $D_s^+ \rightarrow f_0(980)e^+\nu_e$ with $f_0(980) \rightarrow \pi^+\pi^-$ to be $(1.72 \pm 0.13_{\text{stat}} \pm 0.10_{\text{syst}}) \times 10^{-3}$, which is 2.6 times more accurate than the previous measurement [26]. In the $q\bar{q}$ mixture picture, this implies that the $s\bar{s}$ component dominates for the $f_0(980)$. An upper limit on the BF is set to be $\mathcal{B}[D_s^+ \rightarrow f_0(500)e^+\nu_e, f_0(500) \rightarrow \pi^+\pi^-] < 3.3 \times 10^{-4}$ at 90% confidence level with estimation of the negligible nonresonance contribution. Moreover, these BF measurements, especially the one involving the $f_0(500)$, favor the predictions [14,15] of models assuming the $f_0(980)$ and $f_0(500)$ as tetraquark composition over those based on the $q\bar{q}$ mixture picture. This is consistent with the arena of D^+ semileptonic decays [21].

Furthermore, we determine $f_+^{f_0}(0)|V_{cs}| = 0.504 \pm 0.017_{\text{stat}} \pm 0.035_{\text{syst}}$ for the first time by analyzing the dynamics of $D_s^+ \rightarrow f_0(980)e^+\nu_e, f_0(980) \rightarrow \pi^+\pi^-$ decay. Using $|V_{cs}| = 0.97349 \pm 0.00016$ [4], we obtain $f_+^{f_0}(0) = 0.518 \pm 0.018_{\text{stat}} \pm 0.036_{\text{syst}}$. In Table I, the measured form factor result at $q^2 = 0$ is compared with different theoretical predictions. Our measurement agrees with the predictions in Refs. [6–8], but is much higher than the predictions in Refs. [9,11,12]. It is notable that most predictions for the form factor $f_+^{f_0}(0)$ and BF depend on the angle ϕ , which is only known with large uncertainty. So, the measured form factor and BF are both important to constrain this angle and probe the quark component in $f_0(980)$ [11]. Although most theoretical predictions for $f_+^{f_0}(0)$ have a large uncertainty due to the ϕ uncertainty, the measured form factor line shape is a powerful tool to distinguish different models. Finally, these results are important to understand the nature of the light scalar states $f_0(980)$ and $f_0(500)$, and the nonperturbative dynamics of charm meson decays.

TABLE I. Comparison of the form factor at $q^2 = 0$ between our measurement and various theoretical predictions (CLFD: covariant light-front dynamics; DR: dispersion relation; QCDSR: QCD sum rule; LCSR: light-cone QCD sum rules; LFQM: light-front quark model; CCQM: covariant confined quark model).

	This work	CLFD [6]	DR [6]	QCDSR [7]	QCDSR [8]	LCSR [9]	LFQM [11]	CCQM [12]
$f_+^{f_0}(0)$	$0.518 \pm 0.018_{\text{stat}} \pm 0.036_{\text{sys}}$	0.45	0.46	0.50 ± 0.13	0.48 ± 0.23	0.30 ± 0.03	0.24 ± 0.05	0.36 ± 0.02
Difference (σ)	...	1.7	1.4	0.1	0.2	4.3	4.3	2.8
ϕ in theory	...	$(32 \pm 4.8)^\circ$	$(41.3 \pm 5.5)^\circ$	35°	$(8_{-8}^{+21})^\circ$...	$(56 \pm 7)^\circ$	31°

The BESIII Collaboration thanks the staff of BEPCII and the IHEP computing center for their strong support. The authors are grateful to De-Liang Yao, Shan Cheng and Xian-Wei Kang for valuable discussions. This work is supported in part by National Key R&D Program of China under Contracts No. 2020YFA0406400, No. 2023YFA1606000, No. 2020YFA0406300; National Natural Science Foundation of China (NSFC) under Contracts No. 11635010, No. 11735014, No. 11835012, No. 11935015, No. 11935016, No. 11935018, No. 11961141012, No. 12022510, No. 12025502, No. 12035009, No. 12035013, No. 12061131003, No. 12192260, No. 12192261, No. 12192262, No. 12192263, No. 12192264, No. 12192265; Natural Science Foundation of Hunan Province, China under Contract No. 2021JJ40036 and the Fundamental Research Funds for the Central Universities under Contract No. 020400/531118010467; the Chinese Academy of Sciences (CAS) Large-Scale Scientific Facility Program; the CAS Center for Excellence in Particle Physics (CCEPP); Joint Large-Scale Scientific Facility Funds of the NSFC and CAS under Contract No. U1832207; CAS Key Research Program of Frontier Sciences under Contracts No. QYZDJ-SSW-SLH003, No. QYZDJ-SSW-SLH040; 100 Talents Program of CAS; The Institute of Nuclear and Particle Physics (INPAC) and Shanghai Key Laboratory for Particle Physics and Cosmology; ERC under Contract No. 758462; European Union's Horizon 2020 research and innovation programme under Marie Skłodowska-Curie grant agreement under Contract No. 894790; German Research Foundation DFG under Contracts No. 443159800, No. 455635585, Collaborative Research Center CRC 1044, FOR5327, GRK 2149; Istituto Nazionale di Fisica Nucleare, Italy; Ministry of Development of Turkey under Contract No. DPT2006K-120470; National Research Foundation of Korea under Contract No. NRF-2022R1A2C1092335; National Science and Technology Fund of Mongolia; National Science Research and Innovation Fund (NSRF) via the Program Management Unit for Human Resources and Institutional Development, Research and Innovation of Thailand under Contract No. B16F640076; Polish National Science Centre under Contract No. 2019/35/O/ST2/02907; The Royal Society, UK under Contract No. DH160214; The Swedish Research Council; U.S. Department of Energy under Contract No. DE-FG02-05ER41374.

Appendix A: Introduction to the tag technique.—The semileptonic D_s^+ decays can be studied with a tag technique in the process $e^+e^- \rightarrow D_s^{*\pm} D_s^\mp \rightarrow \gamma D_s^+ D_s^-$ where the neutrino is only undetected in the final states. There are two types of samples used in the tag technique: tag sample and double tag sample. In the tag sample, the D_s^- mesons are reconstructed through various hadronic decays. In the double tag sample appropriately designated as the “signal” sample in this Letter, besides the tag D_s^- , the semileptonic signal D_s^+ and the transition photon from the decay $D_s^{*\pm} \rightarrow \gamma D_s^\pm$ reconstructed with the remaining charged tracks and neutral showers. The BF with this tag technique is obtained with the following formula:

$$\mathcal{B}_{\text{sig}} = \frac{N_{\text{sig}}^{\text{tot}}}{\mathcal{B}_\gamma \times \sum_i N_{\text{tag}}^i \times (\epsilon_{\text{tag,sig}}^i / \epsilon_{\text{tag}}^i)} = \frac{N_{\text{sig}}^{\text{tot}}}{\mathcal{B}_\gamma \times N_{\text{tag}}^{\text{tot}} \times \bar{\epsilon}}, \quad (\text{A1})$$

where N_{tag}^i , ϵ_{tag}^i , and $\epsilon_{\text{tag,sig}}^i$ are tag yield, tag efficiency, and signal efficiency with the present tag for the i th tag mode, respectively; \mathcal{B}_γ is the BF of $D_s^{*\pm} \rightarrow \gamma D_s^\pm$ decay; $\bar{\epsilon} = \sum_i [(N_{\text{tag}}^i / N_{\text{tag}}^{\text{tot}}) \times (\epsilon_{\text{tag,sig}}^i / \epsilon_{\text{tag}}^i)]$ is the weighted efficiency.

Appendix B: Systematic uncertainties of the BF measurement.—For the decay $D_s^+ \rightarrow f_0(980)e^+\nu_e$ with $f_0(980) \rightarrow \pi^+\pi^-$, there are the below systematic uncertainties of the BF measurement. The systematic uncertainties of the tracking or particle identification efficiencies of π^\pm and e^+ are studied with control samples of $e^+e^- \rightarrow K^+K^-\pi^+\pi^-$ and $e^+e^- \rightarrow \gamma e^+e^-$ processes. For e^+ and π^\pm , both the tracking and particle identification uncertainties are assigned to be 0.5% and 1.0% for the $\pi^+\pi^-$ pair. The uncertainty from the quoted BF of $D_s^{*\pm} \rightarrow \gamma D_s^\pm$ decay is 0.7% [4]. The uncertainty due to the transition photon reconstruction is estimated to be 2.0% using the control sample of $e^+e^- \rightarrow D_s^{*\pm} D_s^\mp$ events, where D_s^- decays via a tag mode, while D_s^+ decays via one of the two hadronic channels: $D_s^+ \rightarrow K_S^0 K^+$ or $D_s^+ \rightarrow K^+ K^- \pi^+$. The uncertainty in the total number of the tag D_s^- mesons is assigned to be 0.3% by examining the changes of the fit yields when varying the signal shape, background shape, and taking into account the background fluctuation in the fit. The uncertainty associated with the signal MC model is estimated to be 4.4% by replacing the $f_0(980)$ line shape from BESII

[39] with the one from LHCb [48] in generating the signal MC samples. The uncertainty of the $M_{\pi^+\pi^-}$ fit is estimated to be 2.1% by altering the nominal MC background shape. Firstly, we use alternative MC shapes where the relative fractions of backgrounds from continuum and non- $D_s^{\pm}D_s^{\mp}$ open-charm processes are varied by $\pm 30\%$ according to the uncertainties of their assigned cross sections in the inclusive MC sample. Secondly, we vary the relative fraction ($\pm 1\sigma$) of the peaking background channel $D_s^+ \rightarrow \eta'(\gamma\pi^+\pi^-)e^+\nu_e$ [4]. The uncertainty due to neglecting other S -wave contributions was found to be negligible. The total systematic uncertainty is 5.6%, obtained by adding all contributions in quadrature.

For the decay $D_s^+ \rightarrow f_0(500)e^+\nu_e$ with $f_0(500) \rightarrow \pi^+\pi^-$, there are two types of systematic uncertainties of the upper limit on the BF measurement: additive and multiplicative. The additive uncertainty is dominated by the background shape. Besides the same uncertainty sources following the previous BF measurement, we change the relative fraction ($\pm 1\sigma$) of the major background of $D_s^+ \rightarrow \eta e^+\nu_e$ decay [4] and the peak background of $D_s^+ \rightarrow f_0(980)e^+\nu_e$ decay. The multiplicative uncertainties are the same as those for $D_s^+ \rightarrow f_0(980)e^+\nu_e$ decay except for the signal MC model efficiency. This uncertainty is estimated to be 1.1% by varying the parameters of the Bugg line shape [49] within their uncertainties in generating the signal MC samples.

-
- [1] J. R. Pelaez, *Phys. Rep.* **658**, 1 (2016).
 [2] W. Wang and C. D. Lu, *Phys. Rev. D* **82**, 034016 (2010).
 [3] R. L. Jaffe, *Phys. Rev. D* **15**, 267 (1977).
 [4] R. L. Workman *et al.* (Particle Data Group), *Prog. Theor. Exp. Phys.* **2022**, 083C01 (2022).
 [5] V. V. Anisovich, L. Montanet, and V. N. Nikonov, *Phys. Lett. B* **480**, 19 (2000).
 [6] B. El-Bennich, O. Leitner, J. P. Dedonder, and B. Loiseau, *Phys. Rev. D* **79**, 076004 (2009).
 [7] I. Bediaga, F. S. Navarra, and M. Nielsen, *Phys. Lett. B* **579**, 59 (2004).
 [8] T. M. Aliev and M. Savci, *Europhys. Lett.* **90**, 61001 (2010).
 [9] P. Colangelo, F. De Fazio, and W. Wang, *Phys. Rev. D* **81**, 074001 (2010).
 [10] Y. J. Shi and W. Wang, *Phys. Rev. D* **92**, 074038 (2015).
 [11] H. W. Ke, X. Q. Li, and Z. T. Wei, *Phys. Rev. D* **80**, 074030 (2009).
 [12] N. R. Soni, A. N. Gadaria, J. J. Patel, and J. N. Pandya, *Phys. Rev. D* **102**, 016013 (2020).
 [13] S. Cheng and J. M. Shen, *Eur. Phys. J. C* **80**, 554 (2020).
 [14] R. M. Wang, Y. Qiao, Y. J. Zhang, X. D. Cheng, and Y. G. Xu, *Phys. Rev. D* **107**, 056022 (2023).
 [15] Y. K. Hsiao, S. Q. Yang, W. J. Wei, and B. C. Ke, arXiv:2306.06091.
 [16] J. R. Peláez, *Phys. Rev. Lett.* **92**, 102001 (2004); N. N. Achasov and A. V. Kiselev, *Phys. Rev. D* **73**, 054029 (2006); G. 't Hooft, G. Isidori, L. Maiani, A. D. Polosa, and V. Riquer, *Phys. Lett. B* **662**, 424 (2008); A. H. Fariborz, R. Jora, and J. Schechter, *Phys. Rev. D* **79**, 074014 (2009); S. Weinberg, *Phys. Rev. Lett.* **110**, 261601 (2013); H. C. Kim, K. S. Kim, M. K. Cheoun, Daisuke Jido, and Makoto Oka, *Phys. Rev. D* **99**, 014005 (2019).
 [17] J. Weinstein and N. Isgur, *Phys. Rev. D* **41**, 2236 (1990); T. Branz, T. Gutschea, and V. Lyubovitskij, *Eur. Phys. J. A* **37**, 303 (2008); L. Y. Dai, X. G. Wang, and H. Q. Zheng, *Commun. Theor. Phys.* **58**, 410 (2012); L. Y. Dai and M. R. Pennington, *Phys. Lett. B* **736**, 11 (2014); T. Sekihara and S. Kumano, *Phys. Rev. D* **92**, 034010 (2015); D. L. Yao, L. Y. Dai, H. Q. Zheng, and Z. Y. Zhou, *Rep. Prog. Phys.* **84**, 076201 (2021); Z. Q. Wang, X. W. Kang, J. A. Oller, and L. Zhang, *Phys. Rev. D* **105**, 074016 (2022).
 [18] N. N. Achasov and A. V. Kiselev, *Phys. Rev. D* **86**, 114010 (2012).
 [19] T. Sekihara and E. Oset, *Phys. Rev. D* **92**, 054038 (2015).
 [20] M. Ablikim *et al.* (BESIII Collaboration), *Phys. Rev. Lett.* **121**, 081802 (2018).
 [21] M. Ablikim *et al.* (BESIII Collaboration), *Phys. Rev. Lett.* **122**, 062001 (2019).
 [22] M. Ablikim *et al.* (BESIII Collaboration), *Phys. Rev. D* **105**, L031101 (2022).
 [23] M. Ablikim *et al.* (BESIII Collaboration), *Phys. Rev. D* **103**, 092004 (2021).
 [24] J. Yelton *et al.* (CLEO Collaboration), *Phys. Rev. D* **80**, 052007 (2009).
 [25] K. M. Ecklund *et al.* (CLEO Collaboration), *Phys. Rev. D* **80**, 052009 (2009).
 [26] J. Hietala, D. Cronin-Hennessy, T. Pedlar, and I. Shipsey, *Phys. Rev. D* **92**, 012009 (2015).
 [27] M. Ablikim *et al.* (BESIII Collaboration), *Phys. Rev. Lett.* **122**, 061801 (2019).
 [28] See Supplemental Material at <http://link.aps.org/supplemental/10.1103/PhysRevLett.132.141901> for additional analysis information.
 [29] M. Ablikim *et al.* (BESIII Collaboration), *Nucl. Instrum. Methods Phys. Res., Sect. A* **614**, 345 (2010).
 [30] M. Ablikim *et al.* (BESIII Collaboration), *Chin. Phys. C* **44**, 040001 (2020).
 [31] X. Li *et al.*, *Radiat. Detect. Technol. Methods* **1**, 13 (2017); Y. X. Guo *et al.*, *Radiat. Detect. Technol. Methods* **1**, 15 (2017).
 [32] S. Agostinelli *et al.* (GEANT4 Collaboration), *Nucl. Instrum. Methods Phys. Res., Sect. A* **506**, 250 (2003).
 [33] K. X. Huang *et al.*, *Nucl. Sci. Tech.* **33**, 142 (2022).
 [34] S. Jadach, B. F. L. Ward, and Z. Was, *Comput. Phys. Commun.* **130**, 260 (2000); *Phys. Rev. D* **63**, 113009 (2001).
 [35] D. J. Lange, *Nucl. Instrum. Methods Phys. Res., Sect. A* **462**, 152 (2001); R. G. Ping, *Chin. Phys. C* **32**, 599 (2008).
 [36] J. C. Chen, G. S. Huang, X. R. Qi, D. H. Zhang, and Y. S. Zhu, *Phys. Rev. D* **62**, 034003 (2000); R. L. Yang, R. G. Ping, and H. Chen, *Chin. Phys. Lett.* **31**, 061301 (2014).
 [37] E. Richter-Was, *Phys. Lett. B* **303**, 163 (1993).
 [38] M. Ablikim *et al.* (BESIII Collaboration), *Phys. Rev. D* **94**, 032001 (2016).
 [39] M. Ablikim *et al.* (BES Collaboration), *Phys. Lett. B* **607**, 243 (2005).

[40] M. Ablikim *et al.* (BESIII Collaboration), *J. High Energy Phys.* **04** (2022) 058.
 [41] M. Ablikim *et al.* (BESIII Collaboration), *Phys. Rev. D* **92**, 071101(R) (2015).
 [42] R. Aaij *et al.* (LHCb Collaboration), *Phys. Rev. D* **87**, 052001 (2013).
 [43] W. Wang, *Phys. Lett. B* **759**, 501 (2016). The form of our double differential decay rate is a little different but consistent with this reference by redefining the parameters of Flattè formula.
 [44] D. Becirevic and A. B. Kaidalov, *Phys. Lett. B* **478**, 417 (2000).
 [45] N. N. Achasov, A. V. Kiselev, and G. N. Shestakov, *Phys. Rev. D* **102**, 016022 (2020).
 [46] R. Aaij *et al.* (LHCb Collaboration), *Phys. Rev. Lett.* **119**, 101801 (2017).
 [47] M. Ablikim *et al.* (BESIII Collaboration), *Phys. Rev. D* **92**, 072012 (2015).
 [48] R. Aaij *et al.* (LHCb Collaboration), *Phys. Rev. D* **86**, 052006 (2012).
 [49] D. V. Bugg, *J. Phys. G* **34**, 151 (2007).

M. Ablikim,¹ M. N. Achasov,^{13,b} P. Adlarson,⁷⁵ R. Aliberti,³⁶ A. Amoroso,^{74a,74c} M. R. An,⁴⁰ Q. An,^{71,58} Y. Bai,⁵⁷ O. Bakina,³⁷ I. Balossino,^{30a} Y. Ban,^{47,g} V. Batozskaya,^{1,45} K. Begzsuren,³³ N. Berger,³⁶ M. Berlowski,⁴⁵ M. Bertani,^{29a} D. Bettoni,^{30a} F. Bianchi,^{74a,74c} E. Bianco,^{74a,74c} J. Bloms,⁶⁸ A. Bortone,^{74a,74c} I. Boyko,³⁷ R. A. Briere,⁵ A. Brueggemann,⁶⁸ H. Cai,⁷⁶ X. Cai,^{1,58} A. Calcaterra,^{29a} G. F. Cao,^{1,63} N. Cao,^{1,63} S. A. Cetin,^{62a} J. F. Chang,^{1,58} T. T. Chang,⁷⁷ W. L. Chang,^{1,63} G. R. Che,⁴⁴ G. Chelkov,^{37,a} C. Chen,⁴⁴ Chao Chen,⁵⁵ G. Chen,¹ H. S. Chen,^{1,63} M. L. Chen,^{1,58,63} S. J. Chen,⁴³ S. M. Chen,⁶¹ T. Chen,^{1,63} X. R. Chen,^{32,63} X. T. Chen,^{1,63} Y. B. Chen,^{1,58} Y. Q. Chen,³⁵ Z. J. Chen,^{26,h} W. S. Cheng,^{74c} S. K. Choi,¹⁰ X. Chu,⁴⁴ G. Cibinetto,^{30a} S. C. Coen,⁴ F. Cossio,^{74c} J. J. Cui,⁵⁰ H. L. Dai,^{1,58} J. P. Dai,⁷⁹ A. Dbeyssi,¹⁹ R. E. de Boer,⁴ D. Dedovich,³⁷ Z. Y. Deng,¹ A. Denig,³⁶ I. Denysenko,³⁷ M. Destefanis,^{74a,74c} F. De Mori,^{74a,74c} B. Ding,^{66,1} X. X. Ding,^{47,g} Y. Ding,³⁵ Y. Ding,⁴¹ J. Dong,^{1,58} L. Y. Dong,^{1,63} M. Y. Dong,^{1,58,63} X. Dong,⁷⁶ S. X. Du,⁸¹ Z. H. Duan,⁴³ P. Egorov,^{37,a} Y. L. Fan,⁷⁶ J. Fang,^{1,58} S. S. Fang,^{1,63} W. X. Fang,¹ Y. Fang,¹ R. Farinelli,^{30a} L. Fava,^{74b,74c} F. Feldbauer,⁴ G. Felici,^{29a} C. Q. Feng,^{71,58} J. H. Feng,⁵⁹ K. Fischer,⁶⁹ M. Fritsch,⁴ C. Fritsch,⁶⁸ C. D. Fu,¹ J. L. Fu,⁶³ Y. W. Fu,¹ H. Gao,⁶³ Y. N. Gao,^{47,g} Yang Gao,^{71,58} S. Garbolino,^{74c} I. Garzia,^{30a,30b} P. T. Ge,⁷⁶ Z. W. Ge,⁴³ C. Geng,⁵⁹ E. M. Gersabeck,⁶⁷ A. Gilman,⁶⁹ K. Goetzen,¹⁴ L. Gong,⁴¹ W. X. Gong,^{1,58} W. Gradl,³⁶ S. Gramigna,^{30a,30b} M. Greco,^{74a,74c} M. H. Gu,^{1,58} Y. T. Gu,¹⁶ C. Y. Guan,^{1,63} Z. L. Guan,²³ A. Q. Guo,^{32,63} L. B. Guo,⁴² R. P. Guo,⁴⁹ Y. P. Guo,^{12,f} A. Guskov,^{37,a} X. T. Hou,^{1,63} T. T. Han,⁵⁰ W. Y. Han,⁴⁰ X. Q. Hao,²⁰ F. A. Harris,⁶⁵ K. K. He,⁵⁵ K. L. He,^{1,63} F. H. Heinsius,⁴ C. H. Heinz,³⁶ Y. K. Heng,^{1,58,63} C. Herold,⁶⁰ T. Holtmann,⁴ P. C. Hong,^{12,f} G. Y. Hou,^{1,63} Y. R. Hou,⁶³ Z. L. Hou,¹ H. M. Hu,^{1,63} J. F. Hu,^{56,i} T. Hu,^{1,58,63} Y. Hu,¹ G. S. Huang,^{71,58} K. X. Huang,⁵⁹ L. Q. Huang,^{32,63} X. T. Huang,⁵⁰ Y. P. Huang,¹ T. Hussain,⁷³ N. Hüsken,^{28,36} W. Imoehl,²⁸ M. Irshad,^{71,58} J. Jackson,²⁸ S. Jaeger,⁴ S. Janchiv,³³ J. H. Jeong,¹⁰ Q. Ji,¹ Q. P. Ji,²⁰ X. B. Ji,^{1,63} X. L. Ji,^{1,58} Y. Y. Ji,⁵⁰ Z. K. Jia,^{71,58} P. C. Jiang,^{47,g} S. S. Jiang,⁴⁰ T. J. Jiang,¹⁷ X. S. Jiang,^{1,58,63} Y. Jiang,⁶³ J. B. Jiao,⁵⁰ Z. Jiao,²⁴ S. Jin,⁴³ Y. Jin,⁶⁶ M. Q. Jing,^{1,63} T. Johansson,⁷⁵ X. Kui,¹ S. Kabana,³⁴ N. Kalantar-Nayestanaki,⁶⁴ X. L. Kang,⁹ X. S. Kang,⁴¹ R. Kappert,⁶⁴ M. Kavatsyuk,⁶⁴ B. C. Ke,⁸¹ A. Khoukaz,⁶⁸ R. Kiuchi,¹ R. Kliemt,¹⁴ L. Koch,³⁸ O. B. Kolcu,^{62a} B. Kopf,⁴ M. K. Kuessner,⁴ A. Kupsc,^{45,75} W. Kühn,³⁸ J. J. Lane,⁶⁷ J. S. Lange,³⁸ P. Larin,¹⁹ A. Lavania,²⁷ L. Lavezzi,^{74a,74c} T. T. Lei,^{71,k} Z. H. Lei,^{71,58} H. Leithoff,³⁶ M. Lellmann,³⁶ T. Lenz,³⁶ C. Li,⁴⁸ C. Li,⁴⁴ C. H. Li,⁴⁰ Cheng Li,^{71,58} D. M. Li,⁸¹ F. Li,^{1,58} G. Li,¹ H. Li,^{71,58} H. B. Li,^{1,63} H. J. Li,²⁰ H. N. Li,^{56,i} Hui Li,⁴⁴ J. R. Li,⁶¹ J. S. Li,⁵⁹ J. W. Li,⁵⁰ Ke Li,¹ L. J. Li,^{1,63} L. K. Li,¹ Lei Li,³ M. H. Li,⁴⁴ P. R. Li,^{39,j,k} S. X. Li,¹² T. Li,⁵⁰ W. D. Li,^{1,63} W. G. Li,¹ X. H. Li,^{71,58} X. L. Li,⁵⁰ Xiaoyu Li,^{1,63} Y. G. Li,^{47,g} Z. J. Li,⁵⁹ Z. X. Li,¹⁶ Z. Y. Li,⁵⁹ C. Liang,⁴³ H. Liang,^{71,58} H. Liang,³⁵ H. Liang,^{1,63} Y. F. Liang,⁵⁴ Y. T. Liang,^{32,63} G. R. Liao,¹⁵ L. Z. Liao,⁵⁰ J. Libby,²⁷ A. Limphirat,⁶⁰ D. X. Lin,^{32,63} T. Lin,¹ B. J. Liu,¹ B. X. Liu,⁷⁶ C. Liu,³⁵ C. X. Liu,¹ D. Liu,^{19,71} F. H. Liu,⁵³ Fang Liu,¹ Feng Liu,⁶ G. M. Liu,^{56,i} H. Liu,^{39,j,k} H. B. Liu,¹⁶ H. M. Liu,^{1,63} Huanhuan Liu,¹ Huihui Liu,²² J. B. Liu,^{71,58} J. L. Liu,⁷² J. Y. Liu,^{1,63} K. Liu,¹ K. Y. Liu,⁴¹ Ke Liu,²³ L. Liu,^{71,58} L. C. Liu,⁴⁴ Lu Liu,⁴⁴ M. H. Liu,^{12,f} P. L. Liu,¹ Q. Liu,⁶³ S. B. Liu,^{71,58} T. Liu,^{12,f} W. K. Liu,⁴⁴ W. M. Liu,^{71,58} X. Liu,^{39,j,k} Y. Liu,^{39,j,k} Y. B. Liu,⁴⁴ Z. A. Liu,^{1,58,63} Z. Q. Liu,⁵⁰ X. C. Lou,^{1,58,63} F. X. Lu,⁵⁹ H. J. Lu,²⁴ J. G. Lu,^{1,58} X. L. Lu,¹ Y. Lu,⁷ Y. P. Lu,^{1,58} Z. H. Lu,^{1,63} C. L. Luo,⁴² M. X. Luo,⁸⁰ T. Luo,^{12,f} X. L. Luo,^{1,58} X. R. Lyu,⁶³ Y. F. Lyu,⁴⁴ F. C. Ma,⁴¹ H. L. Ma,¹ J. L. Ma,^{1,63} L. L. Ma,⁵⁰ M. M. Ma,^{1,63} Q. M. Ma,¹ R. Q. Ma,^{1,63} R. T. Ma,⁶³ X. Y. Ma,^{1,58} Y. Ma,^{47,g} Y. M. Ma,³² F. E. Maas,¹⁹ M. Maggiora,^{74a,74c} S. Maldaner,⁴ S. Malde,⁶⁹ A. Mangoni,^{29b} Y. J. Mao,^{47,g} Z. P. Mao,¹ S. Marcello,^{74a,74c} Z. X. Meng,⁶⁶ J. G. Messchendorp,^{14,64} G. Mezzadri,^{30a} H. Miao,^{1,63} T. J. Min,⁴³ R. E. Mitchell,²⁸ X. H. Mo,^{1,58,63} N. Yu. Muchnoi,^{13,b} Y. Nefedov,³⁷ F. Nerling,^{19,d} I. B. Nikolaev,^{13,b} Z. Ning,^{1,58} S. Nisar,^{11,l} Y. Niu,⁵⁰ S. L. Olsen,⁶³ Q. Ouyang,^{1,58,63} S. Pacetti,^{29b,29c} X. Pan,⁵⁵ Y. Pan,⁵⁷ A. Pathak,³⁵ P. Patteri,^{29a} Y. P. Pei,^{71,58} M. Pelizaeus,⁴ H. P. Peng,^{71,58} K. Peters,^{14,d}

J. L. Ping,⁴² R. G. Ping,^{1,63} S. Plura,³⁶ S. Pogodin,³⁷ V. Prasad,³⁴ F. Z. Qi,¹ H. Qi,^{71,58} H. R. Qi,⁶¹ M. Qi,⁴³ T. Y. Qi,^{12,f} S. Qian,^{1,58} W. B. Qian,⁶³ C. F. Qiao,⁶³ J. J. Qin,⁷² L. Q. Qin,¹⁵ X. P. Qin,^{12,f} X. S. Qin,⁵⁰ Z. H. Qin,^{1,58} J. F. Qiu,¹ S. Q. Qu,⁶¹ C. F. Redmer,³⁶ K. J. Ren,⁴⁰ A. Rivetti,^{74c} V. Rodin,⁶⁴ M. Rolo,^{74c} G. Rong,^{1,63} Ch. Rosner,¹⁹ S. N. Ruan,⁴⁴ N. Salone,⁴⁵ A. Sarantsev,^{37,c} Y. Schelhaas,³⁶ K. Schoenning,⁷⁵ M. Scodreggio,^{30a,30b} K. Y. Shan,^{12,f} W. Shan,²⁵ X. Y. Shan,^{71,58} J. F. Shangguan,⁵⁵ L. G. Shao,^{1,63} M. Shao,^{71,58} C. P. Shen,^{12,f} H. F. Shen,^{1,63} W. H. Shen,⁶³ X. Y. Shen,^{1,63} B. A. Shi,⁶³ H. C. Shi,^{71,58} J. L. Shi,¹² J. Y. Shi,¹ Q. Q. Shi,⁵⁵ R. S. Shi,^{1,63} X. Shi,^{1,58} J. J. Song,²⁰ T. Z. Song,⁵⁹ W. M. Song,^{35,1} Y. J. Song,¹² Y. X. Song,^{47,g} S. Sosio,^{74a,74c} S. Spataro,^{74a,74c} F. Stieler,³⁶ Y. J. Su,⁶³ G. B. Sun,⁷⁶ G. X. Sun,¹ H. Sun,⁶³ H. K. Sun,¹ J. F. Sun,²⁰ K. Sun,⁶¹ L. Sun,⁷⁶ S. S. Sun,^{1,63} T. Sun,^{1,63} W. Y. Sun,³⁵ Y. Sun,⁹ Y. J. Sun,^{71,58} Y. Z. Sun,¹ Z. T. Sun,⁵⁰ Y. X. Tan,^{71,58} C. J. Tang,⁵⁴ G. Y. Tang,¹ J. Tang,⁵⁹ Y. A. Tang,⁷⁶ L. Y. Tao,⁷² Q. T. Tao,^{26,h} M. Tat,⁶⁹ J. X. Teng,^{71,58} V. Thoren,⁷⁵ W. H. Tian,⁵⁹ W. H. Tian,⁵² Y. Tian,^{32,63} Z. F. Tian,⁷⁶ I. Uman,^{62b} B. Wang,¹ B. L. Wang,⁶³ Bo Wang,^{71,58} C. W. Wang,⁴³ D. Y. Wang,^{47,g} F. Wang,⁷² H. J. Wang,^{39,j,k} H. P. Wang,^{1,63} K. Wang,^{1,58} L. L. Wang,¹ M. Wang,⁵⁰ Meng Wang,^{1,63} S. Wang,^{12,f} S. Wang,^{39,j,k} T. Wang,^{12,f} T. J. Wang,⁴⁴ W. Wang,⁵⁹ W. Wang,⁷² W. H. Wang,⁷⁶ W. P. Wang,^{71,58} X. Wang,^{47,g} X. F. Wang,^{39,j,k} X. J. Wang,⁴⁰ X. L. Wang,^{12,f} Y. Wang,⁶¹ Y. D. Wang,⁴⁶ Y. F. Wang,^{1,58,63} Y. H. Wang,⁴⁸ Y. N. Wang,⁴⁶ Y. Q. Wang,¹ Yaqian Wang,^{18,1} Yi Wang,⁶¹ Z. Wang,^{1,58} Z. L. Wang,⁷² Z. Y. Wang,^{1,63} Ziyi Wang,⁶³ D. Wei,⁷⁰ D. H. Wei,¹⁵ F. Weidner,⁶⁸ S. P. Wen,¹ C. W. Wenzel,⁴ U. W. Wiedner,⁴ G. Wilkinson,⁶⁹ M. Wolke,⁷⁵ L. Wollenberg,⁴ C. Wu,⁴⁰ J. F. Wu,^{1,63} L. H. Wu,¹ L. J. Wu,^{1,63} X. Wu,^{12,f} X. H. Wu,³⁵ Y. Wu,⁷¹ Y. J. Wu,³² Z. Wu,^{1,58} L. Xia,^{71,58} X. M. Xian,⁴⁰ T. Xiang,^{47,g} D. Xiao,^{39,j,k} G. Y. Xiao,⁴³ H. Xiao,^{12,f} S. Y. Xiao,¹ Y. L. Xiao,^{12,f} Z. J. Xiao,⁴² C. Xie,⁴³ X. H. Xie,^{47,g} Y. Xie,⁵⁰ Y. G. Xie,^{1,58} Y. H. Xie,⁶ Z. P. Xie,^{71,58} T. Y. Xing,^{1,63} C. F. Xu,^{1,63} C. J. Xu,⁵⁹ G. F. Xu,¹ H. Y. Xu,⁶⁶ Q. J. Xu,¹⁷ Q. N. Xu,³¹ W. Xu,^{1,63} W. L. Xu,⁶⁶ X. P. Xu,⁵⁵ Y. C. Xu,⁷⁸ Z. P. Xu,⁴³ Z. S. Xu,⁶³ F. Yan,^{12,f} L. Yan,^{12,f} W. B. Yan,^{71,58} W. C. Yan,⁸¹ X. Q. Yan,¹ H. J. Yang,^{51,e} H. L. Yang,³⁵ H. X. Yang,¹ Tao Yang,¹ Y. Yang,^{12,f} Y. F. Yang,⁴⁴ Y. X. Yang,^{1,63} Yifan Yang,^{1,63} Z. W. Yang,^{39,j,k} M. Ye,^{1,58} M. H. Ye,⁸ J. H. Yin,¹ Z. Y. You,⁵⁹ B. X. Yu,^{1,58,63} C. X. Yu,⁴⁴ G. Yu,^{1,63} J. S. Yu,^{26,h} T. Yu,⁷² X. D. Yu,^{47,g} C. Z. Yuan,^{1,63} L. Yuan,² S. C. Yuan,¹ X. Q. Yuan,¹ Y. Yuan,^{1,63} Z. Y. Yuan,⁵⁹ C. X. Yue,⁴⁰ A. A. Zafar,⁷³ F. R. Zeng,⁵⁰ X. Zeng,^{12,f} Y. Zeng,^{26,h} Y. J. Zeng,^{1,63} X. Y. Zhai,³⁵ Y. H. Zhan,⁵⁹ A. Q. Zhang,^{1,63} B. L. Zhang,^{1,63} B. X. Zhang,¹ D. H. Zhang,⁴⁴ G. Y. Zhang,²⁰ H. Zhang,⁷¹ H. H. Zhang,⁵⁹ H. H. Zhang,³⁵ H. Q. Zhang,^{1,58,63} H. Y. Zhang,^{1,58} J. J. Zhang,⁵² J. L. Zhang,²¹ J. Q. Zhang,⁴² J. W. Zhang,^{1,58,63} J. X. Zhang,^{39,j,k} J. Y. Zhang,¹ J. Z. Zhang,^{1,63} Jianyu Zhang,⁶³ Jiawei Zhang,^{1,63} L. M. Zhang,⁶¹ L. Q. Zhang,⁵⁹ Lei Zhang,⁴³ P. Zhang,¹ Q. Y. Zhang,^{40,81} Shuihan Zhang,^{1,63} Shulei Zhang,^{26,h} X. D. Zhang,⁴⁶ X. M. Zhang,¹ X. Y. Zhang,⁵⁰ X. Y. Zhang,⁵⁵ Y. Zhang,⁶⁹ Y. Zhang,⁷² Y. T. Zhang,⁸¹ Y. H. Zhang,^{1,58} Yan Zhang,^{71,58} Yao Zhang,¹ Z. H. Zhang,¹ Z. L. Zhang,³⁵ Z. Y. Zhang,⁴⁴ Z. Y. Zhang,⁷⁶ G. Zhao,¹ J. Zhao,⁴⁰ J. Y. Zhao,^{1,63} J. Z. Zhao,^{1,58} Lei Zhao,^{71,58} Ling Zhao,¹ M. G. Zhao,⁴⁴ S. J. Zhao,⁸¹ Y. B. Zhao,^{1,58} Y. X. Zhao,^{32,63} Z. G. Zhao,^{71,58} A. Zhemchugov,^{37,a} B. Zheng,⁷² J. P. Zheng,^{1,58} W. J. Zheng,^{1,63} Y. H. Zheng,⁶³ B. Zhong,⁴² X. Zhong,⁵⁹ H. Zhou,⁵⁰ L. P. Zhou,^{1,63} X. Zhou,⁷⁶ X. K. Zhou,⁶ X. R. Zhou,^{71,58} X. Y. Zhou,⁴⁰ Y. Z. Zhou,^{12,f} J. Zhu,⁴⁴ K. Zhu,¹ K. J. Zhu,^{1,58,63} L. Zhu,³⁵ L. X. Zhu,⁶³ S. H. Zhu,⁷⁰ S. Q. Zhu,⁴³ T. J. Zhu,^{12,f} W. J. Zhu,^{12,f} Y. C. Zhu,^{71,58} Z. A. Zhu,^{1,63} J. H. Zou,¹ and J. Zu^{71,58}

(BESIII Collaboration)

¹*Institute of High Energy Physics, Beijing 100049, People's Republic of China*

²*Beihang University, Beijing 100191, People's Republic of China*

³*Beijing Institute of Petrochemical Technology, Beijing 102617, People's Republic of China*

⁴*Bochum Ruhr-University, D-44780 Bochum, Germany*

⁵*Carnegie Mellon University, Pittsburgh, Pennsylvania 15213, USA*

⁶*Central China Normal University, Wuhan 430079, People's Republic of China*

⁷*Central South University, Changsha 410083, People's Republic of China*

⁸*China Center of Advanced Science and Technology, Beijing 100190, People's Republic of China*

⁹*China University of Geosciences, Wuhan 430074, People's Republic of China*

¹⁰*Chung-Ang University, Seoul, 06974, Republic of Korea*

¹¹*COMSATS University Islamabad, Lahore Campus, Defence Road, Off Raiwind Road, 54000 Lahore, Pakistan*

¹²*Fudan University, Shanghai 200433, People's Republic of China*

¹³*G.I. Budker Institute of Nuclear Physics SB RAS (BINP), Novosibirsk 630090, Russia*

¹⁴*GSI Helmholtzcentre for Heavy Ion Research GmbH, D-64291 Darmstadt, Germany*

¹⁵*Guangxi Normal University, Guilin 541004, People's Republic of China*

- ¹⁶Guangxi University, Nanning 530004, People's Republic of China
- ¹⁷Hangzhou Normal University, Hangzhou 310036, People's Republic of China
- ¹⁸Hebei University, Baoding 071002, People's Republic of China
- ¹⁹Helmholtz Institute Mainz, Staudinger Weg 18, D-55099 Mainz, Germany
- ²⁰Henan Normal University, Xinxiang 453007, People's Republic of China
- ²¹Henan University, Kaifeng 475004, People's Republic of China
- ²²Henan University of Science and Technology, Luoyang 471003, People's Republic of China
- ²³Henan University of Technology, Zhengzhou 450001, People's Republic of China
- ²⁴Huangshan College, Huangshan 245000, People's Republic of China
- ²⁵Hunan Normal University, Changsha 410081, People's Republic of China
- ²⁶Hunan University, Changsha 410082, People's Republic of China
- ²⁷Indian Institute of Technology Madras, Chennai 600036, India
- ²⁸Indiana University, Bloomington, Indiana 47405, USA
- ^{29a}INFN Laboratori Nazionali di Frascati, INFN Laboratori Nazionali di Frascati, I-00044, Frascati, Italy
- ^{29b}INFN Sezione di Perugia, I-06100, Perugia, Italy
- ^{29c}University of Perugia, I-06100, Perugia, Italy
- ^{30a}INFN Sezione di Ferrara, INFN Sezione di Ferrara, I-44122, Ferrara, Italy
- ^{30b}University of Ferrara, I-44122, Ferrara, Italy
- ³¹Inner Mongolia University, Hohhot 010021, People's Republic of China
- ³²Institute of Modern Physics, Lanzhou 730000, People's Republic of China
- ³³Institute of Physics and Technology, Peace Avenue 54B, Ulaanbaatar 13330, Mongolia
- ³⁴Instituto de Alta Investigación, Universidad de Tarapacá, Casilla 7D, Arica, Chile
- ³⁵Jilin University, Changchun 130012, People's Republic of China
- ³⁶Johannes Gutenberg University of Mainz, Johann-Joachim-Becher-Weg 45, D-55099 Mainz, Germany
- ³⁷Joint Institute for Nuclear Research, 141980 Dubna, Moscow region, Russia
- ³⁸Justus-Liebig-Universität Giessen, II. Physikalisches Institut, Heinrich-Buff-Ring 16, D-35392 Giessen, Germany
- ³⁹Lanzhou University, Lanzhou 730000, People's Republic of China
- ⁴⁰Liaoning Normal University, Dalian 116029, People's Republic of China
- ⁴¹Liaoning University, Shenyang 110036, People's Republic of China
- ⁴²Nanjing Normal University, Nanjing 210023, People's Republic of China
- ⁴³Nanjing University, Nanjing 210093, People's Republic of China
- ⁴⁴Nankai University, Tianjin 300071, People's Republic of China
- ⁴⁵National Centre for Nuclear Research, Warsaw 02-093, Poland
- ⁴⁶North China Electric Power University, Beijing 102206, People's Republic of China
- ⁴⁷Peking University, Beijing 100871, People's Republic of China
- ⁴⁸Qufu Normal University, Qufu 273165, People's Republic of China
- ⁴⁹Shandong Normal University, Jinan 250014, People's Republic of China
- ⁵⁰Shandong University, Jinan 250100, People's Republic of China
- ⁵¹Shanghai Jiao Tong University, Shanghai 200240, People's Republic of China
- ⁵²Shanxi Normal University, Linfen 041004, People's Republic of China
- ⁵³Shanxi University, Taiyuan 030006, People's Republic of China
- ⁵⁴Sichuan University, Chengdu 610064, People's Republic of China
- ⁵⁵Soochow University, Suzhou 215006, People's Republic of China
- ⁵⁶South China Normal University, Guangzhou 510006, People's Republic of China
- ⁵⁷Southeast University, Nanjing 211100, People's Republic of China
- ⁵⁸State Key Laboratory of Particle Detection and Electronics, Beijing 100049, Hefei 230026, People's Republic of China
- ⁵⁹Sun Yat-Sen University, Guangzhou 510275, People's Republic of China
- ⁶⁰Suranaree University of Technology, University Avenue 111, Nakhon Ratchasima 30000, Thailand
- ⁶¹Tsinghua University, Beijing 100084, People's Republic of China
- ^{62a}Turkish Accelerator Center Particle Factory Group, Istinye University, 34010, Istanbul, Turkey
- ^{62b}Near East University, Nicosia, North Cyprus, 99138, Mersin 10, Turkey
- ⁶³University of Chinese Academy of Sciences, Beijing 100049, People's Republic of China
- ⁶⁴University of Groningen, NL-9747 AA Groningen, The Netherlands
- ⁶⁵University of Hawaii, Honolulu, Hawaii 96822, USA
- ⁶⁶University of Jinan, Jinan 250022, People's Republic of China
- ⁶⁷University of Manchester, Oxford Road, Manchester M13 9PL, United Kingdom
- ⁶⁸University of Muenster, Wilhelm-Klemm-Strasse 9, 48149 Muenster, Germany
- ⁶⁹University of Oxford, Keble Road, Oxford OX13RH, United Kingdom
- ⁷⁰University of Science and Technology Liaoning, Anshan 114051, People's Republic of China
- ⁷¹University of Science and Technology of China, Hefei 230026, People's Republic of China

⁷²*University of South China, Hengyang 421001, People's Republic of China*

⁷³*University of the Punjab, Lahore-54590, Pakistan*

^{74a}*University of Turin and INFN, University of Turin, I-10125, Turin, Italy*

^{74b}*University of Eastern Piedmont, I-15121, Alessandria, Italy*

^{74c}*INFN, I-10125, Turin, Italy*

⁷⁵*Uppsala University, Box 516, SE-75120 Uppsala, Sweden*

⁷⁶*Wuhan University, Wuhan 430072, People's Republic of China*

⁷⁷*Xinyang Normal University, Xinyang 464000, People's Republic of China*

⁷⁸*Yantai University, Yantai 264005, People's Republic of China*

⁷⁹*Yunnan University, Kunming 650500, People's Republic of China*

⁸⁰*Zhejiang University, Hangzhou 310027, People's Republic of China*

⁸¹*Zhengzhou University, Zhengzhou 450001, People's Republic of China*

^aAlso at the Moscow Institute of Physics and Technology, Moscow 141700, Russia.

^bAlso at the Novosibirsk State University, Novosibirsk, 630090, Russia.

^cAlso at the NRC "Kurchatov Institute," PNPI, 188300, Gatchina, Russia.

^dAlso at Goethe University Frankfurt, 60323 Frankfurt am Main, Germany.

^eAlso at Key Laboratory for Particle Physics, Astrophysics and Cosmology, Ministry of Education; Shanghai Key Laboratory for Particle Physics and Cosmology; Institute of Nuclear and Particle Physics, Shanghai 200240, People's Republic of China.

^fAlso at Key Laboratory of Nuclear Physics and Ion-beam Application (MOE) and Institute of Modern Physics, Fudan University, Shanghai 200443, People's Republic of China.

^gAlso at State Key Laboratory of Nuclear Physics and Technology, Peking University, Beijing 100871, People's Republic of China.

^hAlso at School of Physics and Electronics, Hunan University, Changsha 410082, China.

ⁱAlso at Guangdong Provincial Key Laboratory of Nuclear Science, Institute of Quantum Matter, South China Normal University, Guangzhou 510006, China.

^jAlso at Frontiers Science Center for Rare Isotopes, Lanzhou University, Lanzhou 730000, People's Republic of China.

^kAlso at Lanzhou Center for Theoretical Physics, Lanzhou University, Lanzhou 730000, People's Republic of China.

^lAlso at the Department of Mathematical Sciences, IBA, Karachi 75270, Pakistan.